

Decay dynamics of photoexcited alkali chemisorbates: Real-time investigations in the femtosecond regime

M. Bauer,* S. Pawlik, and M. Aeschlimann[†]

Laboratory for Technical Chemistry, ETH Zurich, CH-8092 Zurich, Switzerland

(Received 15 January 1999)

The inelastic decay time of photoexcited cesium and sodium adsorbed on different single-crystal surfaces has been investigated by means of time-resolved two-photon photoemission. Especially in the case of cesium, we observe a surprisingly high lifetime. For Cs/Cu(111) we obtain a value of 15 ± 6 fs. Intra-atomic hybridization, the specific band structure of the substrate, and adsorption site effects may be responsible for this behavior. These different mechanisms are discussed in detail. [S0163-1829(99)09231-0]

I. INTRODUCTION

A very challenging topic in studying adsorbate dynamics on metal surfaces is the investigation of initial steps in reactions initiated by photon-induced electronic excitations. The high density of electronic states, offered as decay channels to excited electrons by the conducting band in a metal, quenches the time scales of these nonthermal processes into the range of just a few femtoseconds. Today, this is the lower limit of time resolution achievable within real-time experiments.

Most of the attention recently paid to photoexcited adsorbate states focuses on the indirect excitation by hot substrate electrons rather than on direct photoinduced excitation. Stimulated by a variety of different femtosecond laser-induced desorption results, several theoretical investigations of hot carrier-induced excitations have been undertaken.¹ It turns out that dynamical properties such as the dephasing or the resonance lifetime T_R of the adsorbate excitation strongly determines the character of the energy transfer from the electronic, e.g., to a vibrational excitation. In addition, the short lifetimes of electron excitations on metal surfaces suggest in general a highly dynamical process, especially with respect to the nucleus motion of the adsorbate.² However, there exists hardly any experimental investigation which can support these studies. The final energy distribution of desorbed molecules, for example, only allows quite moderate conclusions on the progressing steps within the entire desorption mechanism.³⁻⁵ A deeper insight requires a more direct access to the dynamical processes during the initiating steps. This would in a certain sense be the link between theoretical calculations and final-state investigations.

Photoemission is the classical tool to gain insight into the valence electron system of an adsorbate-substrate system. In this case, the linewidth of spectroscopic structures provides information on the dynamical properties of the electron system. In a (one-photon) photoemission experiment mainly the lifetime of the left hole at the sample is probed.⁶ A two-photon photoemission experiment (2PPE) also allows access to dynamical properties of the usually unoccupied intermediate state involved. Especially with the spectroscopy of the surface located image-potential states, this method has proven itself.⁷ However, next to inhomogeneous Gaussian

broadening the complex excitation mechanism in a 2PPE experiment restricts the validity of linewidth measurements.⁸

The extension of two-photon photoemission to a pump and probe mode, that is time-resolved two-photon photoemission (TR-2PPE), enables us to perform a real-time experiment to study the dynamic properties of optically excited electronic states.^{9,10} In fact both methods, linewidth and real-time measurement, simultaneously probe the dephasing of polarization and the inelastic lifetime of the excited electron. Therefore, studies based on a combination of these two methods promise to differentiate to a certain degree between those two dynamic properties. Just recently this approach has been successfully applied in Ref. 11. Under consideration of their 2PPE and TR-2PPE results, the authors were able to consistently describe the dynamical properties of the ($n = 1$) image-potential state as observed on a Cu(111) surface.

In spite of impressive progress in the investigation of the electron dynamics of excited volume and surface metallic states by TR-2PPE,^{12-15,25} the study of the lifetime of electronic adsorbate excitations seems to be still quite challenging. For a chemisorption system the strong coupling between adsorbate excited states and electron-hole pairs of the substrate shortens the lifetime T_R to a few femtoseconds. Hence it is not surprising that TR-2PPE experiments on adsorbate systems have been reported by three groups so far.^{13,16-18} The latter reference is the only one reporting on a lifetime effect as induced by an adsorbate excitation.

In this paper, we extend these results reported for Cs/Cu(111) to different alkali-noble-metal complexes. That is, these are the systems Cs/Cu(100), Na/Cu(100), and Cs/Ag(111). In addition, we applied a method of deeper data analysis on these and our earlier results, which will be discussed in detail. It takes into account the dephasing of the photoinduced excitation steps and, therefore, supplies a more realistic picture of the actual 2PPE excitation process. Further, we were able to measure the decay time of this adsorbate state as function of its energy. The discussion of our results focuses (1) on the mechanism responsible for the quite long lifetime observed, and (2) a comparison of the results obtained for different alkali-noble-metal complexes.

II. 2PPE MODEL AND DATA ANALYSIS

An attempt to model experimental (TR-)2PPE data requires, first of all, a definition of the system we are looking

at. In the present case we are considering an excitation of an electron from a band of occupied metal states into a band of unoccupied states above the vacuum level which couple to our electron detector. This process is induced by the successive absorption of two photons and, in our case, is mediated by an usually unoccupied alkali state at an intermediate energy lying between this two bands and well below the vacuum energy. In each of the four studied systems at the investigated detection angle this intermediate alkali state lies in a projected band gap of the substrate electronic structure. In addition, as the excitation involves the surface-located adsorbate state, a direct excitation into vacuum states [inverse low-energy electron-diffraction (LEED) states] is reasonable.

There might be also some contribution to our signal from the highest occupied alkali orbital acting as initial state, which is known to be located around the Fermi edge. Depending on the respective definition, this state has been shown to be either almost empty at the investigated low coverage or to strongly mix with the bulk conducting band.^{19,20} Both views are in line with the assumption of an initial-state distribution given by an occupied metal band. In the first case any contribution from this state can be assumed to be small compared to contributions from the high-density metal band. In the second case a distinction between metal band and alkali state is not really possible any more.

To simulate a 2PPE spectrum, we considered only contributions to our signal arising from the dominant resonant excitation from initial to final state. This means that the electron population of the final state energy E_{final} has been assumed to arise only from an initial state of the occupied metal band located at exactly $\varepsilon = \hbar\omega_1 + \hbar\omega_2$ below E_{final} , where $\hbar\omega_1$ and $\hbar\omega_2$ correspond to the energies of the two exciting photons. Off-resonant excitation has been neglected. With respect to the intermediate state, however, nonresonant contributions were taken into account. The TR-2PPE data (autocorrelation traces) were only evaluated for the maximum of our 2PPE signal which corresponds in our approach to a resonant excitation between initial state and intermediate (alkali) states as well as intermediate and final states.

A quantum-mechanical attempt to describe the interaction of an electron system and a time-dependent electromagnetic field $\vec{E}(t)$ can be made within the framework of the density-matrix formalism.²³ In order to describe the dynamical processes involved in TR-2PPE, Hertel *et al.* applied this formalism to a two-level system, representing the initial and intermediate states of the 2PPE process.¹⁴ This model can be expanded to a three-level system, corresponding to the initial, intermediate, and final states, interacting with an electromagnetic field.^{21,22} The Liouville–von Neumann equation describes the temporal evolution of the density matrix $\hat{\rho}$:

$$\frac{d}{dt}\hat{\rho} = -\frac{i}{\hbar}[\hat{H}, \hat{\rho}] + \frac{d}{dt}\hat{\rho}^{\text{diss}}, \quad (1)$$

where $\hat{H} = \hat{H}_0 + \hat{V}$, \hat{H}_0 is the Hamilton of the electron system, and \hat{V} the perturbation due to its interaction with the electromagnetic field. The off-diagonal elements of the density matrix $\hat{\rho}$ represent the optically induced coherence between two states, whereas the diagonal elements correspond to the population of the respective states. The dissipative terms in these equations take into account the interaction of

the electronic three-level system with a thermal bath, as offered, e.g., by a surrounding electron gas. It gives rise to phase loss between electron and exciting photon field as well as to energy loss of excited electrons. In a dipole approximation, the elements of \hat{H} are given by

$$(\hat{H})_{ij} = \vec{E}(t) \cdot \vec{\mu}_{ij} \quad \text{for } i \neq j,$$

$$(\hat{H})_{ii} = E_i.$$

$\vec{\mu}_{ij}$ is the dipole moment given by $\langle i | \vec{r} | j \rangle$. $E_i = \hbar\omega_i$ is defined by $\hat{H}_0 | i \rangle = E_i | i \rangle$. We define $\phi_{ij}(t) \equiv (1/\hbar) \cdot \vec{\mu}_{ij} \cdot \vec{E}(t)$. The value of ϕ_{ij} is a measure for the strength of the respective optical transition.

In the case of a three-level system we obtain a set of nine coupled differential equations:

$$\frac{d}{dt}\rho_{11} = -i\phi_{12}(\rho_{21} - \rho_{12}) + \frac{d}{dt}\rho_{11}^{\text{diss}}, \quad (2)$$

$$\frac{d}{dt}\rho_{22} = -i \cdot [\phi_{12}(\rho_{12} - \rho_{21}) + \phi_{23}(\rho_{32} - \rho_{23})] + \frac{d}{dt}\rho_{22}^{\text{diss}}, \quad (3)$$

$$\frac{d}{dt}\rho_{33} = -i\phi_{23}(\rho_{23} - \rho_{32}) + \frac{d}{dt}\rho_{33}^{\text{diss}}, \quad (4)$$

$$\frac{d}{dt}\rho_{13} = -i(\phi_{12}\rho_{23} - \phi_{23}\rho_{12}) + i(\omega_1 - \omega_3)\rho_{13} + \frac{d}{dt}\rho_{13}^{\text{diss}}, \quad (5)$$

$$\begin{aligned} \frac{d}{dt}\rho_{12} = & -i\phi_{12}(\rho_{22} - \rho_{11}) + i\phi_{23} \cdot \rho_{13} \\ & + i(\omega_1 - \omega_2)\rho_{12} + \frac{d}{dt}\rho_{12}^{\text{diss}}, \end{aligned} \quad (6)$$

$$\begin{aligned} \frac{d}{dt}\rho_{23} = & -i\phi_{23}(\rho_{33} - \rho_{22}) - i\phi_{12}\rho_{13} \\ & + i(\omega_2 - \omega_3)\rho_{23} + \frac{d}{dt}\rho_{23}^{\text{diss}}, \end{aligned} \quad (7)$$

$$\frac{d}{dt}\rho_{ij} = \frac{d}{dt}\rho_{ji}^* \quad \text{for } i \neq j. \quad (8)$$

In this representation, direct coupling between initial and final states has been neglected ($\phi_{13} = 0$). The dissipative off-diagonal terms $(d/dt)\rho_{ij}^{\text{diss}}$ are due to phase decay during an excitation between $|i\rangle$ and $|j\rangle$, and are given by

$$\begin{aligned} \frac{d}{dt}\rho_{ij}^{\text{diss}} = & -\Gamma_{ij}\rho_{ij}, \\ \Gamma_{ij} = & \Gamma_i + \Gamma_j. \end{aligned} \quad (9)$$

Here Γ_i and Γ_j are the phase loss rates of the involved electronic wave functions, induced by elastic- and inelastic-scattering processes as a result of interaction with the bath. $(d/dt)\rho_{ii}^{\text{diss}}$ accounts for the population and depopulation of

the states due to the inelastic-scattering processes. Assuming that relaxation of electrons can occur only by decay into the ground state $|1\rangle$, we have

$$\frac{d}{dt}\rho_{11}^{\text{diss}} = \frac{1}{T_R}\rho_{22} + \frac{1}{T_{\text{final}}}\rho_{33},$$

$$\frac{d}{dt}\rho_{22}^{\text{diss}} = -\frac{1}{T_R}\rho_{22},$$

$$\frac{d}{dt}\rho_{33}^{\text{diss}} = -\frac{1}{T_{\text{final}}}\rho_{33}.$$

Here T_R and T_{final} are the lifetimes of the intermediate state $|2\rangle$ and final state $|3\rangle$ due to inelastic decay. If only these inelastic-scattering processes contribute to the phase loss of a wave function, its dephasing rate is given by $\Gamma = (1/2T)$.²³ Therefore, T determines the minimum phase loss rate. Any other contribution, such as defect/impurity scattering or (nearly elastic) electron-phonon scattering, would increase Γ (additional, pure dephasing).

For weak excitation densities as used in the present work the initial state density remains nearly one during the whole excitation and deexcitation process, $(d/dt)\rho_{11}^{\text{diss}} \approx 0$. This means that it makes no difference if we consider a closed three-level system with respect to particle conservation or if excited electrons can also decay into empty states offered by the surrounding electron system.

In comparison to a model based on the assumption that the 2PPE process is correctly described by Fermi's golden rule, the density-matrix formalism is a more realistic description of the dynamical process of our 2PPE experiment.²³ Fermi's golden Rule correctly describes an excitation process for $\Delta E \gg 2\pi\hbar/t \gg \delta E$, where ΔE is the width of the final-state distribution, δE the state separation in the final-state distribution, and t the duration of the excitation process.²⁴ These conditions are no longer met for an excitation into a discrete state at a time scale of 40 fs, as in our case given by the width of the exciting laser pulse.

Our simulations of 2PPE spectra and TR-2PPE data were calculated by assuming a temporal evolution of the electromagnetic field of the form $\vec{E}(t) = E_0[\vec{e}_1 g(t/\tau_0)\cos(\omega t)]$ with $g(t/\tau) = [\pi \cosh(t/\tau_0)]^{-1}$. Here $g^2(t/\tau_0)$ is the intensity envelope of the exciting laser pulse, and τ_0 the temporal width of the laser pulse [$\tau_0 = 0.5673\tau_{1/2}$, with $\tau_{1/2}$ the full width at half maximum (FWHM) of the pulse shape]. For a simulation of a time-resolved experiment, pump and probe pulse have to be considered, and therefore $\vec{E}(t) = \vec{E}_0 \cdot g(t/\tau_1)\cos(\omega t) + \vec{E}_0 g[(t+\Delta)/\tau_2]\cos[\omega(t+\Delta)]$. Here Δ is the temporal delay between the pump and probe pulses. This form accounts for the fact that for the present study single color and equal intensity 2PPE modes have been used. The dipole moments of the different excitation steps were assumed to be equal and independent of initial- and final-state energy. The product of the optical transition strength, ϕ_{ij} and the pulse width $\tau_{1/2}$ is a measure of the achievable populations in the respective states during an excitation process. To account for the small transition probabilities in our (TR-)2PPE experiment and to avoid saturation effects during the simulation, the product $\phi_{ij}\tau_{1/2}$ was chosen to be small compared to π , a

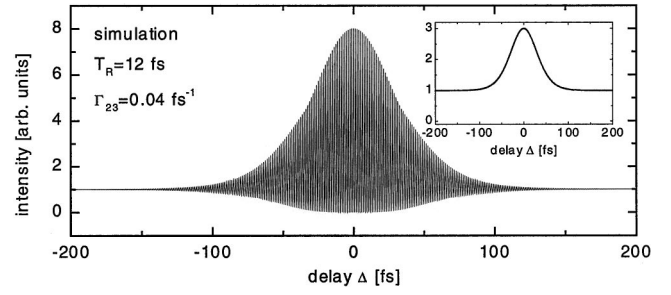


FIG. 1. Calculated autocorrelation trace for a monochromatic equal-polarized pump and probe experiment using the density-matrix formalism. The peak-to-background ratio of the interferometric trace is 8:1. For data analysis we compare the experimental data with the Fourier-filtered trace, as shown in the inset.

critical value with respect to inversion of population.²³ Figure 1 displays a numerical solution for typical parameters as used to simulate our experimental autocorrelation traces. As with the used experimental setup no resolution of the interferometric interaction between pump and probe pulses could be achieved, for comparison, the high-frequency contributions of the simulated traces were filtered out by Fourier filtering. The resulting trace is shown in the inset.

To fit our experimental traces by means of solutions of Eqs. (2)–(8) we first attempted to make reasonable assumptions on as many of the five dynamical parameters ($T_R, T_{\text{final}}, \Gamma_{12}, \Gamma_{23}, \Gamma_{13}$) as possible. Taking into account Eq. (9) we can in any case approximate $\Gamma_{ij} \approx \Gamma_i$ as long as $\Gamma_i \gg \Gamma_j$. This becomes important as soon as one of the dephasing rates is below our temporal resolution, which is mainly determined by the temporal width of the exciting laser pulse of about 40 fs (rapid dephasing). Any dynamical parameter, which is sufficiently small compared to our pulse width, does not change the shape of our autocorrelation signal. Our computer simulations confirm this (obvious) behavior. In detail we observe that time scales below 2 fs of each of the five free parameters show no significant change in the detailed shape of the simulated autocorrelation traces, and cannot be resolved in our experiment. It acts on our measured signal like an instantaneous decay.

In contrast to this, the simulated 2PPE spectra can be quite sensitive to changes even at high dephasing rates. It turns out that Γ_{13} plays just a minor role, whereas the line-width and shape are mainly determined by Γ_{12} and Γ_{23} . We find, however, that as long as the dephasing rates of these two quantities are sufficiently different, the spectrum is mainly determined by the *lowest* dephasing rate (see Fig. 2).

In our experiment a rapid phase loss seems to be reasonable for the initial state $|1\rangle$ of the 2PPE excitation process as long as we assume that it is a bulk state of the metallic substrate. The strong coupling of bulk states to phonons and bulk electronic states should give rise to sufficiently high dephasing rates.¹⁴ As a result, Γ_1 reduces the values of Γ_{12} and Γ_{13} to the range of rapid dephasing. In our calculations we set $\Gamma_{12} = \Gamma_{13} = 1 \text{ fs}^{-1}$.

A further parameter that we were able to fix is the inelastic depopulation time T_{final} in the 2PPE experiment. Considering the shape of our simulations, we did not observe any dependence on this parameter. For convenience we chose a vanishing decay rate for the final state population (T_{final}

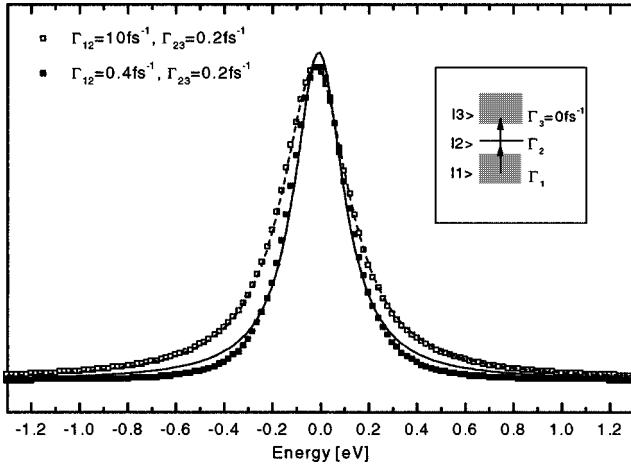


FIG. 2. 2PPE spectra, calculated by means of the Liouville–von Neumann equations. Here the energy zero corresponds to the position of the intermediate state $|2\rangle$. The squares correspond to values of the numerical solutions, and the unbroken and dashed lines are fits of a Lorentzian into these data. Rapid dephasing within the first excitation step at sufficiently low dephasing rate within the second step ($\Gamma_{12} \gg \Gamma_{23}$) results in a FWHM determined by Γ_{23} (open squares). In addition, the pulse shape is Lorentzian. In the case of $\Gamma_{12} \approx \Gamma_{23}$ the pulse width cannot be correlated to one of the dephasing rates (solid squares). This also results in a distortion of the Lorentzian shape. The inset schematically displays the assumed excitation mechanism involving a band of initial and final states and a discrete state located inside a band gap.

$\rightarrow \infty$). Assuming a 2PPE excitation process from a surface-located intermediate adsorbate state into a certainly strong bulk-decoupled vacuum state (inverse LEED state) this choice seems to be reasonable.

Two remaining (free) parameters are left. The first is the inelastic lifetime of the intermediate level T_R , corresponding to the depopulation of the adsorbate excitation, which is the quantity we are interested in. The second parameter is the phase loss rate Γ_{23} of the second excitation step from the adsorbate state into the vacuum. Within limits, we can make statements about the value of the latter quantity. In the event that Γ_{23} is exclusively determined by the inelastic decay of the intermediate state (no “pure” dephasing due to elastic processes), the phase loss rate is given by $\Gamma_{23} = 1/2T_R$. Any further contribution will increase its value. On the other hand, assuming a rapid phase loss of the initial state ($\Gamma_{12} \gg \Gamma_{23}$), the upper limit of Γ_{23} can be deduced from the line-width of the corresponding peak appearing in the 2PPE spectrum.

To evaluate the inelastic lifetime T_R of the cesium excitation, we calculated a set of autocorrelation traces for these two limiting cases of Γ_{23} to fit the measured trace. A small value of Γ_{23} thereby gives rise to a broadening of the autocorrelation trace and reduces the fitted depopulation time T_R , whereas the upper limit of Γ_{23} determines the upper value of T_R . Table I summarizes the assumptions on the dynamical parameters used for data fitting.

III. EXPERIMENT

The laser system used for our TR-2PPE experiments was a mode-locked Ti:sapphire laser, pumped by about 9 W from

TABLE I. Dynamical parameters we chose to simulate the excitation process of cesium adsorbed on Cu(111) by means of the Liouville–von Neumann equations for different T_R (and Γ_{23}).

Γ_{12}	Γ_{13}	T_3	Γ_{23}	T_R
$> 1 \text{ fs}^{-1}$	$> 1 \text{ fs}^{-1}$	$\rightarrow \infty$	$(2 * T_R)^{-1} >$ $\Gamma_{23} > 0.17 \text{ fs}^{-1}$	to be adjusted

a cw Ar⁺ laser. The system delivers transform-limited and sech² temporally shaped pulses of up to 15 nJ/pulse with a pulse width (FWHM) of 40 fs and a repetition rate of 82 MHz. The wavelength can be tuned to a range of 740–830 nm. The linearly polarized output of the Ti:sapphire laser is frequency doubled in a 0.2-mm-thick beta barium borate crystal to produce UV pulses at $h\nu = 3 - 3.4 \text{ eV}$. The conversion rate is about 10% giving pulse energies of up to 1.5 nJ. The UV beam is sent through a pair of fused silica prisms to precompensate for pulse broadening due to dispersive elements such as lenses, beam splitters, and the UHV chamber window in the optical path. A group velocity dispersion (GVD) and intensity loss matched interferometric Mach-Zehnder setup was used for the time-resolved (pump-probe) experiment. The pulses were split by a beam splitter to equal intensity (pump and probe pulses), and one path could be delayed with respect to the other by a computer-controlled delay stage. Before being directed into the UHV chamber both beams were combined colinearly by a second beam splitter. Both beams were focused onto the sample mounted in a UHV chamber with a base pressure of $8 \times 10^{-11} \text{ mbar}$. Photoemitted electrons were detected by a cylindrical sector energy analyzer. Each of the presented time-resolved experiments on adsorbate excitations was performed in the monochromatic autocorrelated mode, both beams being p polarized. To avoid space-charge effects the number of photoemitted electrons per laser pulse were kept in the range of one per pulse. In addition a negative bias of 4 V was applied to the sample. The energy resolution of the analyzer is 80 meV at 4-eV pass energy, and its angular resolution is $\pm 6^\circ$. The system response function of our experimental setup (laser autocorrelation curve) in a time-resolved 2PPE experiment was measured either by direct excitation from an occupied Shockley surface state [in the case of a Cu(111) surface], as described by Hertel *et al.*,¹⁴ or by an excitation from the Fermi edge of a polycrystalline transition metal sheet (in our case molybdenum and tantalum) mounted just below the single crystal sample, as described in Ref. 25.

The following four systems were investigated during our studies of alkali excitations at metal substrates: Cs adsorbed on a Cu(111) single-crystal surface, Cs adsorbed on a Cu(100) single-crystal surface, Na adsorbed on a Cu(100) single-crystal surface, and Cs adsorbed on a Ag(111) single-crystal surface. The copper single crystals were routinely cleaned by repeated argon ion sputtering and annealing (1000 V, 800 K). The sample state was checked by Auger and LEED. The silver sample was made by evaporating *in situ* 60-ML Ag onto the clean (100)-oriented copper single-crystal surface. Silver is known to develop a Ag(111)-like closed film at a coverage of $\theta > 1 \text{ ML}$ on Cu(100).²⁶ We also observed this type of growth mode using LEED and ultraviolet photoemission spectroscopy. The alkali metals (ce-

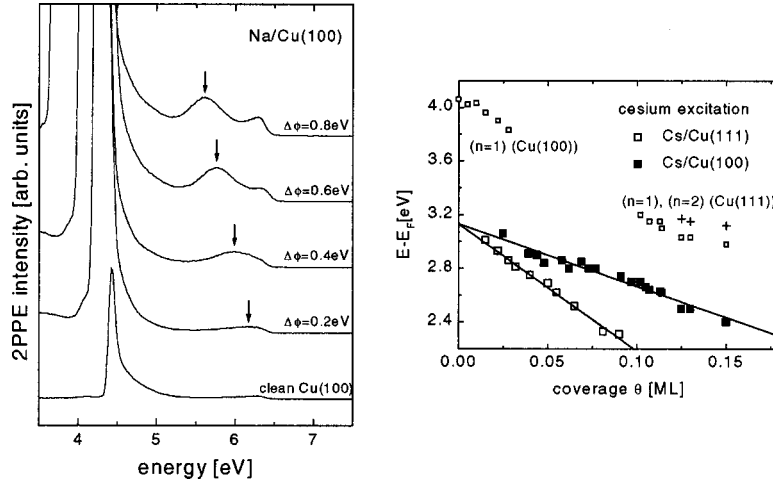


FIG. 3. Left: 2PPE spectra taken for different coverages of sodium adsorbed on Cu(100). The work-function change is due to the increasing number of adsorbed alkali atoms, and serves as a measure for the coverage. The arrow marks the position of the alkali resonance. Right: energy vs coverage dependence of different unoccupied states as observed for cesium adsorbed on Cu(100) and Cu(111). The observation of the ($n=1$) image state of Cu(100) at a coverage below 0.02 ML is possible due to a three-photon photoemission process.

sium and sodium) were deposited by resistive heated getter sources. The pressure during evaporation was maintained in the low- 10^{-10} mbar range. All experiments were performed at room temperature. As the work function of the substrate is very sensitive to alkali adsorption, its change, determined by the onset of the 2PPE spectra, served as a measure of the alkali coverage. In the case of Cs/Cu(111) and Cs/Cu(100), we estimated the absolute coverage by comparing the measured changes in work function with calibration curves $\Delta\phi(\theta)$ in Refs. 27 and 28. No reference data were available for Na/Cu(100) and Cs/Ag(111). However, in our experiments we were in any case in the range of a strongly decreasing work function ϕ with increasing coverage. The observed almost linear dependence of ϕ as function of deposition time indicates that we are in a coverage regime well below 0.5 ML,²⁹ and that interaction of neighboring alkali atoms (due to depolarization fields) is small.³⁰ Upon alkali adsorption a distinct feature appears in the 2PPE spectra for all four investigated systems, which can be attributed to an usually unoccupied electronic state (see Fig. 3). Our data presented here focus on the dynamical properties of this specific excitation. These excited states in alkali-metal complexes had been investigated and characterized by inverse photoemission (IPE) and 2PPE in several publications before. They are usually attributed to electronic excitation of the alkali adsorbate and to be derived from its p_z valence orbital.^{31,32} Its excitation energy (with respect to the Fermi level) shows quite a strong coverage dependence. Below about half a monolayer it shifts by a few eV monotonically toward the Fermi edge with increasing coverage (see Fig. 3, right).³³ This shift is caused by the depolarization field induced by the increasing number of surrounding alkali atoms rather than, for example, by an overlap of the corresponding adsorbate wave functions.³⁰ As a consequence no momentum dispersion of alkali states can be observed at low coverage.³⁴ This point is important to note: the direct interaction between neighboring alkali atoms due to the overlap of their wave function can be neglected at the investigated coverages. No indication for a resonant excitation from an occupied discrete state could be observed, neither under changing excitation

(photon) energy, nor due to the energetical shift as function of coverage. We therefore exclude the 2PPE process to be mediated by an intra-atomic excitation between occupied and unoccupied adsorbate levels. These observations justify the choice of a fast dephasing metal bulk state for the initial state in our simulations.

IV. EXPERIMENTAL RESULTS

A. Cesium adsorbed on Cu(111)

Figure 4 (left) shows a comparison of the FWHM of measured 2PPE autocorrelation traces as a function of electron energy. We obtained these data from a Cu(111) surface covered with 0.08 ML of cesium. For comparison, the results for a clean Cu(111) surface are presented (open circles). The difference between the two measurements is obvious. We observe a pronounced broadening of the autocorrelation traces right in the energy region, where we also observe the peak arising from the unoccupied cesium state in our 2PPE spectra (Fig. 4, right). This raw analysis already indicates a drastic change in the dynamics of an electron when it is excited into an alkali state instead of an excitation into a bulk electronic state of equal energy.

A linewidth analysis of the cesium peak appearing in the 2PPE spectrum limits the dephasing rate Γ_{23} to be below 0.17 fs^{-1} (Fig. 5). Note that the simulations shown have been convoluted with a Gaussian resolution function representing the energy resolution of the electron analyzer of 80 meV. Obviously our simulations only barely fit into the measured trace. This is probably the result of a strong inhomogeneous (Gaussian) contribution in the measured spectrum that we observed and which has been reported for alkali states earlier.^{17,32} As possible source for this broadening one can think, e.g., of the rapid diffusion or vibrational excitations of the alkali-substrate bond at room temperature. We are not able to include such effects into our simulations. Qualitatively, however, this additional broadening means that our linewidth analysis is restricted to an upper limit for Γ_{23} . As already mentioned in Sec. II the linewidth of the state in the

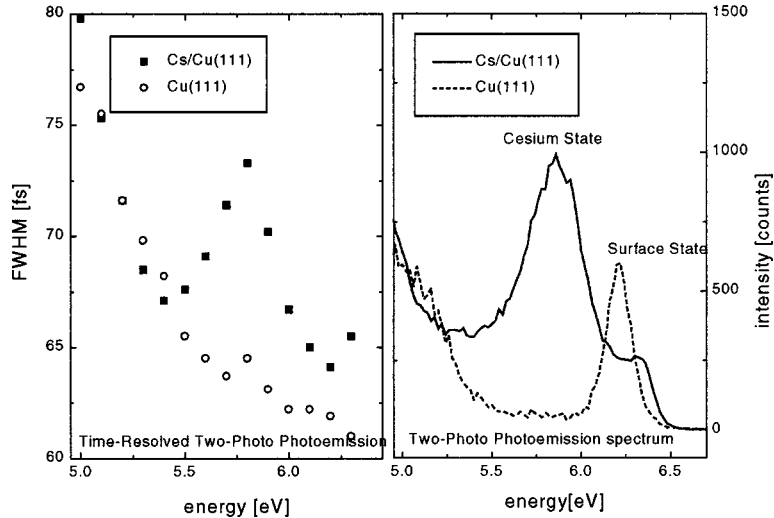


FIG. 4. Full width at half maximum as obtained from the experimental autocorrelation traces of a time-resolved 2PPE experiment and the corresponding 2PPE spectra. Compared to the clean Cu(111) surface, the lifetime data show a pronounced peak in the FWHM of the measured autocorrelation traces, right in the energy region, where we also observe the cesium-induced peak in our 2PPE spectra. This indicates that the dynamical properties of the respective alkali excitation are quite different to those corresponding to bulk electronic excitations. The pronounced peak at 6.2 eV of the clean surface (dashed spectrum) arises from the occupied Shockley surface state. This feature is, however, strongly quenched due to cesium adsorption.

2PPE spectrum also determines the upper value of the inelastic lifetime T_R as obtained using the Liouville–von Neumann fitting routine. Therefore, any way to reduce the inhomogeneous broadening should also result in a reduction of this upper limit for T_R . As mentioned above, the lower limit for the dephasing rate is given by $\Gamma_{23} = 1/2T_R$.

For these two limits of Γ_{23} , Fig. 6 shows the resulting best fits of numerical to experimental autocorrelation traces, at the left for the lower limit of $\Gamma_{23} = 1/2T_R$ and at the right for $\Gamma_{23} = 0.17 \text{ fs}^{-1}$. The traces were obtained at a kinetic energy coinciding with the maximum of the cesium peak in the 2PPE spectrum. For comparison, the open squares indicate the laser autocorrelation trace measured by a nonresonant excitation from the Shockley surface state via a virtual intermediate state of the clean Cu(111) surface. The unbroken line is a fit giving a laser pulse width of 39.5 fs for the pump and the probe pulse under the assumption of a sech^2 pulse shape.

For the lower limit of Γ_{23} an inelastic lifetime T_R for the excited Cs of $12 \pm 3 \text{ fs}$ is acquired, resulting in a $\Gamma_{23} = 1/2T_R = 0.04 \text{ fs}^{-1}$. For the upper limit of Γ_{23} the best fit is obtained by $T_R = 17 \pm 3 \text{ fs}$. Therefore, we conclude the reso-

nance time of the cesium state to be within $T_R = 15 \pm 6 \text{ fs}$. This decay time has to be compared with our estimation of $T_R = 11 \text{ fs}$ given in Ref. 17, which is based on the assumption that the excitation process is sufficiently described within the framework of Fermi's golden rule.

In the following, we present our lifetime data as obtained under assumption of the lowest possible dephasing rate for the second excitation step, which is given by $\Gamma_{23} = 1/2T_R$. As we are mainly interested in comparing changes of lifetime, the following conclusions remain unchanged despite this restriction. Note that an assumption of a higher dephasing rate will result in an extracted higher value of T_R .

B. Dependence of T_R on excitation energy

The lifetime of excited bulk states and image potential states of metals is quite a strong function of their excitation energy. This has been predicted theoretically,^{35,49} and has been demonstrated in a variety of experiments.^{15,36–39}

Little is known, however, about the energy dependence of the lifetime of an excited adsorbate state. But this knowledge could provide insight into the underlying processes for the

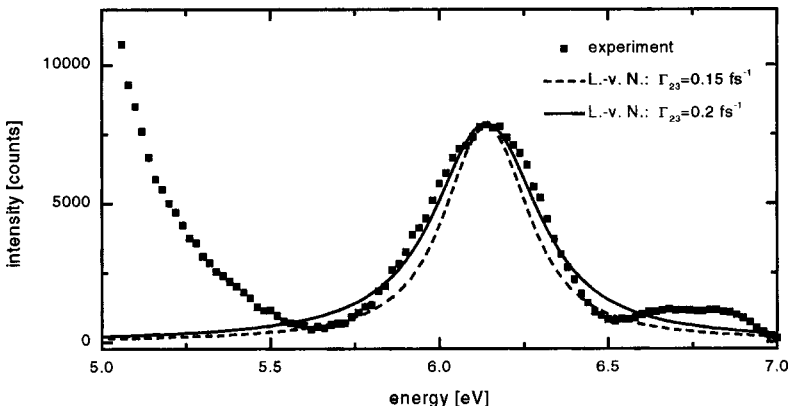


FIG. 5. Estimation of the upper limit of the phase loss rate Γ_{23} of the investigated cesium state on Cu(111); the filled squares correspond to the measured 2PPE spectra corrected by the subtraction of the linear background. Lines are results of our density-matrix simulation convoluted with the resolution function of the used detector for $\Gamma_{23} = 0.15 \text{ fs}^{-1}$ (dashed line) and $\Gamma_{23} = 0.2 \text{ fs}^{-1}$ (unbroken line). The experimental trace is obviously disturbed by an additional strong Gaussian broadening mechanism. We estimate Γ_{23} to be smaller than 0.17 fs^{-1} .

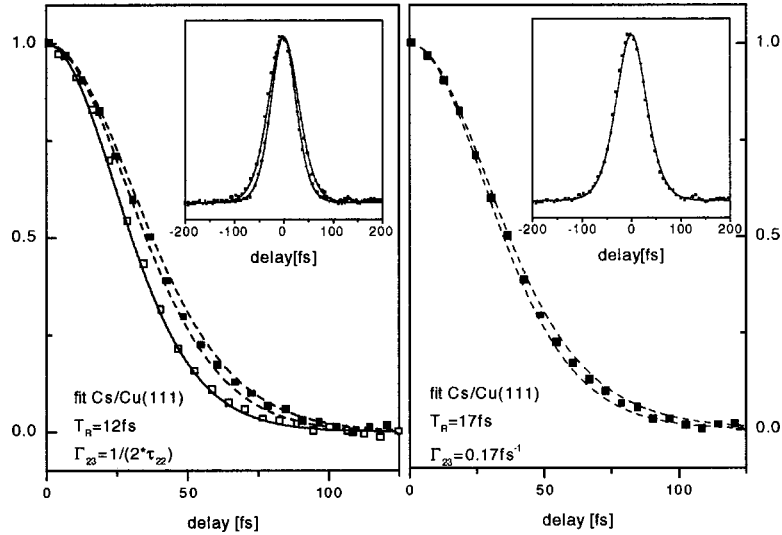


FIG. 6. Data analysis of a time-resolved 2PPE autocorrelation trace as observed for the excited cesium state at a Cu(111) surface. Left: measured autocorrelation trace compared to calculated traces of $T_R=9$ and 14 fs for positive delay, assuming that the dephasing rate Γ_{23} is exclusively determined by T_R (dashed line). The inset shows the complete autocorrelation trace and the solution of the Liouville-von Neumann equations for $T_R=12$ fs. Open squares indicate the laser autocorrelation measured by excitation from the Shockley surface state of the clean Cu(111) surface. The unbroken line is a fit giving a pulse width of 39.5 fs for the two exciting laser pulses. Right: data evaluation based on the assumption that Γ_{23} is determined by the line-width of the Cs peak observed in the 2PPE spectrum. The lines indicate traces calculated for $T_R=14$ and 20 fs.

different decay mechanisms of the resonance state. For example, if a direct interaction with the substrate electronic system (inelastic scattering with substrate electrons) dominates the decay, we expect an analog dependence on $E_{\text{exc}} = E - E_F$ as observed for bulk electronic excitations.

A change of the resonance energy of the alkali state can be realized easily just by changing the alkali coverage, as already explained in some detail in Sec. III. Autocorrelation traces as observed for four different alkali coverages in the Cs/Cu(111) system are shown in Fig. 7. For comparison, the open squares represent the laser autocorrelation trace as measured by a nonresonant excitation from the Shockley surface state of the Cu(111) surface. The inset illustrates the different energetical position of the state with respect to the projected electronic band structure of the copper substrate. Due to the strong one-photon photoemission signal appearing at work

function values ϕ close to $h\nu$, the accessible energy range must be limited to excitation energies $2.4 \text{ eV} < E - E_F < 3.2 \text{ eV}$.

In the tested energy range ($\Delta E = 0.8 \text{ eV}$), we could not trace any change in the inelastic lifetime within our time resolution. The determined lifetime T_R stays within a range of 12 ± 4 fs for all four coverages (at $\Gamma_{23} = 1/2T_R = 0.04 \text{ fs}^{-1}$).

C. Results obtained for other alkali-noble-metal systems

The previous described investigations on Cs/Cu(111) were extended to other alkali-noble-metal complexes. The choice of the different systems was motivated by the potential to control specific complex properties. Our aim was to gain systematically additional information about the

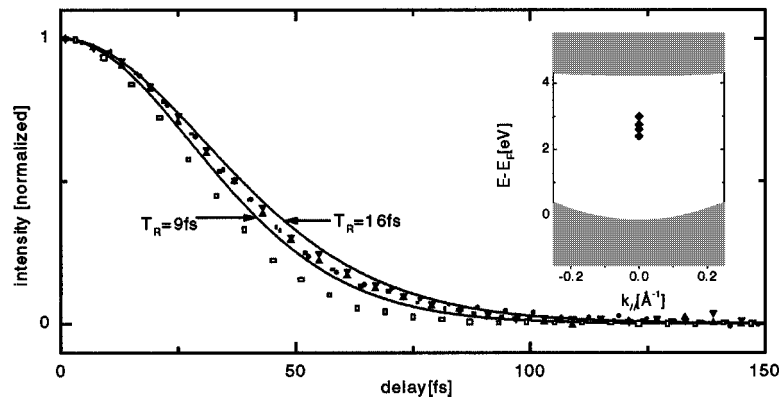


FIG. 7. Lifetime dependence of the cesium excitation as a function of its energetic position with respect to the edges of the sp band gap of the Cu(111) substrate. The filled symbols display autocorrelation traces for positive delay as observed for four different energies within a range of approximately 1 eV (see the inset). The open squares show the measured laser autocorrelation. The lines correspond to simulated traces for $T_R=9$ and 16 fs, respectively [for convenience we assumed $\Gamma_{23} = (2 * T_R)^{-1}$]. The lifetime of the excitation remained constant within ± 4 fs in the investigated energy range.

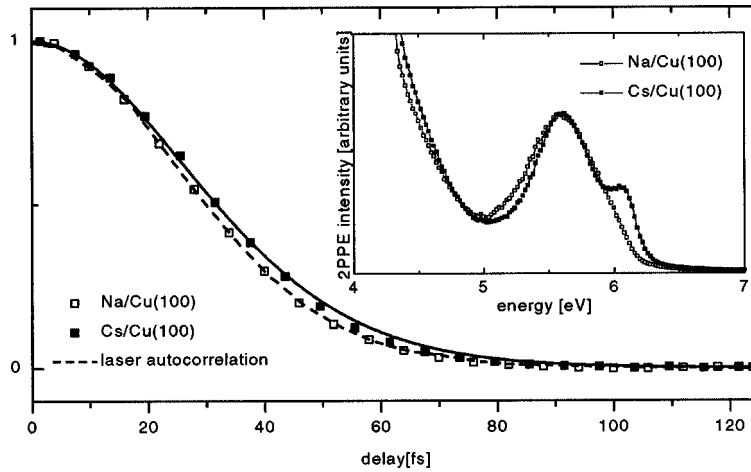


FIG. 8. 2PPE (inset) and TR-2PPE data for the systems Cs/Cu(100) (■) and Na/Cu(100) (□) (positive delay). A comparison of the spectra shows a slight line broadening in the case of Na compared to Cs, already indicating a change in its dynamical behavior. In the case of Cs/Cu(100) we observe an inelastic lifetime of 6 ± 4 fs (simulation given by the solid line), whereas for Na we cannot resolve any difference compared to the measured autocorrelation trace (given by the dashed line).

coupling/decoupling mechanism between alkali atom and substrate. These specific selection were (a) a change of substrate orientation [Cu(111)→Cu(100)], (b) a change of adsorbate (alkali) species (Cs→Na), and (c) a change of substrate species (Cu→Ag). We performed measurements on Cs and Na adsorbed on Cu(100) and Cs adsorbed on Ag(111). For all three systems a very distinct feature arising from an excited alkali state appeared in our 2PPE spectra.

1. Cs/Cu(100) and Na/Cu(100)

Figure 8 displays TR-2PPE results for Cs and Na adsorbed on Cu(100) at the energy coinciding with the corresponding peak in the 2PPE spectra. As presented in the inset, this feature arising from the respective alkali excitation is clearly visible. The autocorrelation traces correspond again to the maximum 2PPE intensity in the insets. To achieve comparable conditions, the sodium and cesium coverages were adjusted so that the excitation appeared at the same energy level. It is clearly visible that the broadening of the autocorrelation trace for Na and Cs/Cu(100) compared to the system response (dashed curve) is much smaller than in the case of Cs/Cu(111) (see Fig. 6). At first sight the inelastic lifetime for those adsorbate species is significantly shorter than for Cs/Cu(111). The numerically extracted inelastic lifetime T_R for Cs/Cu(100) is 6 ± 4 fs. We conclude at this point that a cesium excitation on the Cu(100) surface decays about twice as fast as on the Cu(111) surface. For the adsorbed sodium we were not able to resolve any lifetime effect due to the alkali resonance. As an upper limit for the lifetime a value of 4 fs can be stated.

2. Cs/Ag(111)

For a clean Ag(111) surface a distinct feature appears in the 2PPE spectra arising from direct initial to final state excitation in the bulk. The origin of this peak has been described in an earlier publication in detail.⁴⁰ It is strongly broadened in energy. As shown in Fig. 9(a), the peak remains under alkali adsorption. It clearly overlaps with the electron emission signal from the cesium excitation over the

whole coverage regime we were able to investigate. For increasing electron detection angle (increasing k_{\parallel}), a strong dispersion is observable for the direct excitation in the bulk (see arrow), whereas no dispersion was found within the detected k_{\parallel} range for the excited cesium state.

Figure 9(b) shows TR-2PPE results for Cs adsorbed on Ag(111). The lifetime effect due to the alkali excitation is again quite obvious. A distinct increase in the FWHM of the autocorrelation trace appears in correlation with the alkali peak in the 2PPE spectrum, as observed at 5.5 eV. The contribution from the direct bulk excitation channel restricts, however, our conclusions on the absolute value on the lifetime T_R of the excitation. Figure 9(c) displays the measured FWHM of the autocorrelation trace at 5.5 eV (the maximum of the 2PPE intensity due to the cesium resonance) as function of emission angle. Clearly visible is the decreased FWHM caused by the increased direct excitation contribution to the autocorrelation signal intersecting the cesium resonance. Hence we are only able to give a lower limit for the decay time of the cesium state. The shape of the autocorrelation traces taken at normal emission fit best with the simulated trace for $T_R = 7$ fs ($\Gamma_{23} = 1/2T_R$). The actual resonance time T_R of the cesium excitation, however, is definitively longer and is probably in the range of the lifetime we observed for Cs/Cu(111). The different resonance times of the investigated systems are collected in Table II, as well as the measured linewidth of the corresponding excitation peak in the 2PPE spectrum.

V. DISCUSSION

Such a long lifetime of a photoexcited adsorbate state as observed [for Cs/Cu(111), $T_R \geq 9$ fs] is not necessarily an expected result for a chemisorption system and requires an explanation. Even the experimental linewidth of the observed states in the 2PPE spectra indicates a much longer depopulation times than predicted in theoretical studies. Under the assumption that this state is derived from a pure atomic alkali orbital, linewidths in the range of above 1 eV would be expected, resulting in lifetimes far below 1 fs.^{41,42}

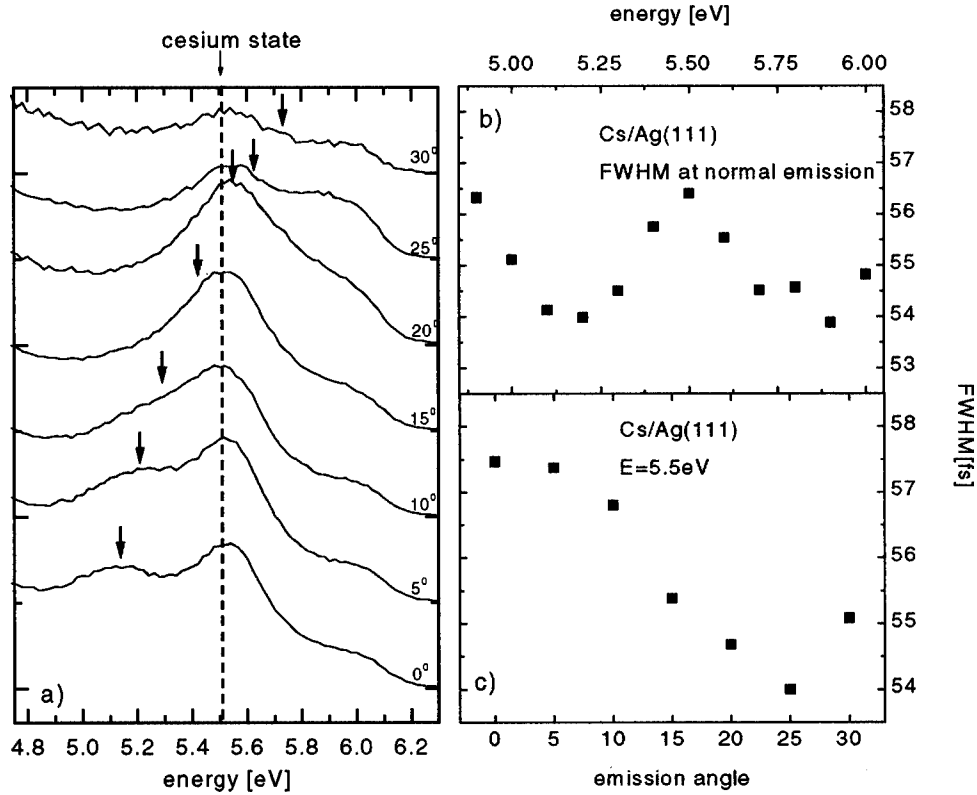


FIG. 9. Experimental results for cesium adsorbed on Ag(111): (a) 2PPE spectra taken at different emission angles. 0° corresponds to normal emission. Note the intersection of the strong dispersing direct excitation with the cesium state. (b) FWHM of autocorrelation traces as a function of measured electron energy at normal emission. The distinct peak appears again at the energy where we also observe the cesium-induced feature in our spectra. (c) FWHM of autocorrelation traces as a function of emission angle at $E=5.5\text{ eV}$ corresponding to the spectra on the right. The influence of the increased direct excitation contribution to the autocorrelation curve is clearly visible in the decay of the FWHM. The minimum is slightly shifted to larger angles than expected from the overlap of direct excitation and alkali state. This is the result of an increased background signal from (short living) bulk excitations at k_{\parallel} values closer to the band-gap edge.

This has to be compared to a measured value of the FWHM being not more than 520 meV for the investigated systems. But this value marks only the lower limit for the actual inelastic lifetime of the resonance state.⁴³

In view of the results as obtained for the $2\pi^*$ resonance of a CO molecule adsorbed on copper single-crystal surfaces, the observed long lifetime of the cesium excitation becomes even more remarkable. The lifetime of this CO excitation still seems to be below the present temporal resolution of TR-2PPE. According to recent experiments the upper limit of T_R is estimated to be at 5 fs.⁴⁴

In Ref. 17 we have already proposed the effect of intratomic hybridization, induced by the surface potential of the substrate, to be a possible explanation for the surprisingly long lifetime of the alkali state. A mixing, for example, of $6s$ and $6p_z$ valence levels of cesium, as proposed first by Muscat and Newns,⁴⁵ induces an orientation of one of the in-

volved states away from the surface into the vacuum. The responsible decoupling from the substrate has to be attributed to the reduced amplitude of the wave function between adsorbate and the surface.⁴² It acts as a tunneling barrier between the metal substrate and the excited cesium state. Experimental evidence for the “binding” counterpart located between surface and alkali adsorbate was actually reported in Ref. 46.

Latest theoretical investigations on the system Cs/Cu(111) seem to confirm the view of hybridization further.⁴⁷ However, the authors concluded that an antibinding character of the cesium state alone would rather result in lifetimes of just 1 fs than of 10 fs. Their calculations indicate that the projected energy band gap of the substrate supports the decoupling due to hybridization and leads to such lifetimes we observe in our experiment. For the Cu(111) surface, for example, the projected band gap exhibits from 0.85 eV below

TABLE II. Inelastic lifetimes as observed for the different systems investigated. For completeness we also add the measured linewidths of the alkali peaks in our 2PPE spectra. Note, however, that the alkali feature cannot be fitted by a Lorentzian, but it contains strong Gaussian contributions.

	Cs/Cu(111)	Cs/Ag(111)	Cs/Cu(100)	Na/Cu(100)
T_R ($\Gamma_{23}=1/2T_R$)	12 ± 3 fs	>7 fs	6 ± 4 fs	<4 fs
FWHM (eV)	350 ± 50 meV	<420 meV	400 ± 50 meV	520 ± 50 meV

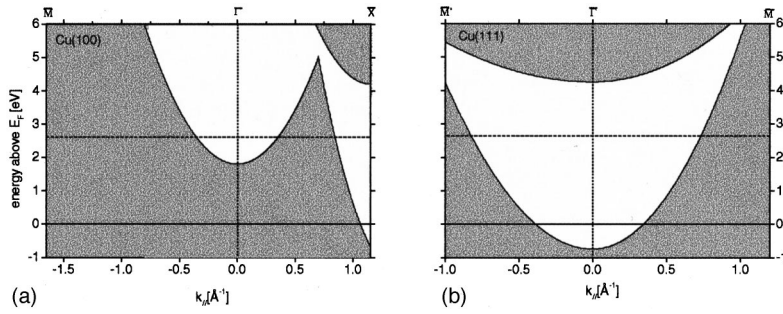


FIG. 10. Projected band structure for (a) Cu(100) and (b) Cu(111). The dashed line indicates an energy level of an excited alkali state at 2.6 eV above E_F . The momentum distance to real bulk states from the band gap center is much smaller for Cu(100) than for Cu(111).

E_F to 4.1 eV above E_F for zero parallel momentum ($k_{\parallel}=0$) at $T=300$ K. The reflecting property of the band gap on electrons at least with momentum around $k_{\parallel}=0$ strongly quenches their interaction with the bulk electronic structure.

A measurement of the 2PPE intensity arising from the alkali excitation as a function of the laser polarization shows that we are dealing with an alkali state which is invariable under rotation around the surface normal.⁴⁸ We conclude that the photoexcited state must be oriented into the z direction (defined as direction perpendicular to the surface). Therefore, in the case of cesium, it is rather reasonable that this excitation is derived from the atomic $6s$, $6p_z$, or $5d_z$ valence level of the free atom (or a mixing of such states). As a result, the minimum separation between adsorbate state and substrate is along the symmetry axis parallel to the surface normal. The barrier transparency to the bulk is the largest along this direction (at $k_{\parallel}=0$). This should be the preferential direction for electron tunneling through the potential barrier separating the atom and the metal. Exactly this decay process is strongly quenched by the location of the projected band gap.⁴⁷

In view of this explanation it is remarkable that no indication for any change in the decay time as function of the resonance energy could be detected for Cs/Cu(111). Such dependence has been theoretically predicted⁴⁹ and also experimentally verified³⁹ for image potential states. Their dynamical properties are also supposed to be strongly correlated with the reflecting property of a band gap. In particular, these states show a very distinct lifetime dependence as a function of their energetical position inside a band gap. In general, the closer these states are located to a band gap edge, the shorter their lifetime is. Next to an edge the penetration of the image state wave function into the bulk is far longer than at the center and, therefore, the coupling to the bulk is strongly increased. In a heuristic approach the first approximation is to set the lifetime inverse proportional to the penetration p into the bulk.^{7,50} For the ($n=1$) image state of Cu(111), for example, a lifetime change of approximately 60 fs has been reported when its energy position is shifted by about 0.5 eV from close to the upper band-gap edge toward the band-gap center.³⁹ In contrast to our observations for the excited cesium state as investigated on a Cu(111) surface, we would expect an increase in the lifetime with decreasing excitation energy (increasing coverage) by moving away from the top edge of the band gap to its center (see Fig. 7).

A significant difference between image potential states and alkali states in the low-coverage regime is, however, their dispersion in k_{\parallel} . Image potential states exhibit a quite strong, nearly free-electron-like dispersion,⁴⁹ whereas for the alkali state at low coverage no dispersion can be observed.³⁴

In contrast to image potential states, a decay of the localized alkali excitation into bulk states can, within the requirement of energy conservation, in principle also occur at quite high values of k_{\parallel} , outside the band gap. As discussed above, the orientation of the alkali state gives rise to an increasing tunneling gap with increasing values of k_{\parallel} . At sufficiently high k values, however, real substrate states become accessible for decay (Fig. 10). Due to the sp -like dispersion of the band-gap edges the distance in k_{\parallel} of real substrate states to the center of the surface Brillouin zone ($k_{\parallel}=0$) is a strong function of energy. It decreases in direction to the bottom of the band gap. With decreasing excitation energy the decay channels to real state become accessible already at lower values of k_{\parallel} (Fig. 10, right). Consequently we expect an increased decay probability and a reduced decay time of the excitation, respectively.⁵¹

There might exist a competition between the energy dependence of the wave-function penetration into the bulk and the momentum dependence of coupling to a real states which hinders us from observing a significant change in the lifetime T_R of the cesium excitation as a function of excitation energy. The assumption that the decay channel at $k_{\parallel}=0$ is by far the dominating decay channel for the cesium excitation might thus be oversimplifying, as contributions at $k_{\parallel}\neq 0$ have to be taken into account.

To compare our results of different alkali adsorption systems, we have to consider different effects on the decay probability of an adsorbate state. A change of substrate geometry [Cu(111) \rightarrow Cu(100)] affects the electron dynamics of the system at least in two ways. As discussed in Sec. IV, the projected band structure of the substrate, mainly the position of a band gap, is a very important parameter in terms of decoupling the alkali excitation from the bulk. The change from a (111)-oriented to a (100)-oriented copper surface means—roughly speaking—an upward shift of the band gap at $k_{\parallel}=0$ by approximately 3 eV (Fig. 10). For a fixed excitation energy, this means a drastic change in the position of the alkali excitation with respect to the band-gap edges. It is not surprising that quite a different behavior in the lifetime T_R of the cesium excitation can be observed. In detail, decay channels to real states are obtainable for much smaller momentum values k_{\parallel} for a Cu(100) surface than for a Cu(111) surface. For example, for an excitation energy of 3 eV the distance from the surface Brillouin center has been reduced from about $k_{\parallel}=0.7$ to 0.4 \AA^{-1} .³⁴ For our experimental conditions also the separation in energy of the band-gap edges is smaller in the case of the (100) surface. The resulting increase in wave-function penetration into the bulk stimulates further the decay of the cesium state.

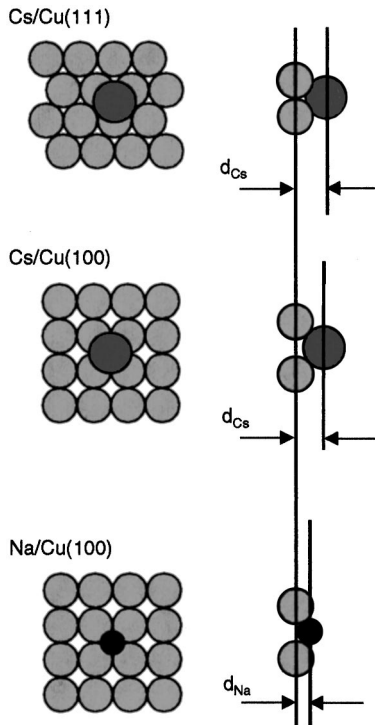


FIG. 11. Schematic sketch of the supposed adsorption sites for the different alkali-metal-metal systems at their highest coordination, as investigated within this work.

In addition the changed adsorption geometry has to be taken into account. The more open structure of the (100)-oriented surface gives way to deeper penetration of the Cs adsorbate into the surface than the closely packed (111) surface would allow (as schematically shown in Fig. 11). Consequently the tunneling barrier between cesium atom and (100)-oriented copper surface is reduced. How effective a change in the actual adsorbate-substrate separation might act on the dynamical properties of an alkali excitation has been shown in a calculation by Muscat and Newns on the $6s$ resonance of Cs chemisorbed on Ni. They found a change in the lifetime “broadening” approximately from 700 to 1200 meV due to an approach of the adsorbate of just 0.2 Å closer to the surface at reasonable chemisorption distances.⁴⁵ This value corresponds to a lifetime reduction by a factor of about 2. These two effects, the changed band-gap position as well as the changed adsorption site, support a decrease in lifetime of the cesium excitation on a Cu(100) substrate compared to a Cu(111) substrate, and is in nice agreement with our observations.

The influence of adsorption geometry on the dynamical properties of alkali excitation might become more evident from the different results observed for Na/Cu(100) and Cs/Cu(100), respectively. Obviously, changes which are due to a differing band structure of the substrate do not have to be taken into account. The question arises, however, whether we are dealing with the same kind of alkali excitation. Considering the intra-atomic hybridization, a sodium atom offers just a $2s$ and a $2p_z$ levels to mix. In the case of cesium, for example, a contribution from the $5d_z$ valence level is also reasonable,⁴² and might change the detailed shape of the excitation wave function compared to the sodium excitation. The almost identical 2PPE spectra of both systems can be

considered as an indication (but surely not as a proof) that the observed peaks for Cs and Na are due to the same excitation. Not only the line shape but also the intensity and coverage dependence we observe for the alkali excitation in both cases are very similar (see Fig. 8). At least this demonstrates that we have detected quite similar types of excitations. In addition, the calculations of Ref. 47 suggest that it is not that much the detailed shape of the wave function (e.g., the strength of hybridization) which is responsible for lifetimes in the regime of several femtoseconds, but the position of the excited alkali state regarding the band gap as well as the overall adsorbate-substrate distance which determines the dynamical properties at these time scales. Therefore, as we have tuned the position of cesium and sodium excitation to the same position within the substrate band gap, we can focus our discussion on the adsorption geometry.

The ionic radius⁵² of sodium is 1.13 Å, compared to 1.81 Å for cesium. It is obvious that this should result in a much deeper penetration into the substrate surface for sodium atoms than for cesium atoms (see Fig. 11). For the metallic radius of a copper atom of 1.28 Å, we estimated the difference in the average adsorbate-substrate separation to be almost 1 Å. Within a simple hard-core model we calculated a distance from the center of the first surface layer of Cu(100) of 1.6 Å for sodium and 2.5 Å for cesium assuming a four-fold hollow adsorption site in both cases. The sodium atom seems to be almost embedded into the Cu(100) surface. A further penetration of the sodium cannot be excluded. For adsorption of Na on Pt(111), even an entire incorporation of the adsorbate into the first substrate layer has been reported for small coverages.⁵³ We expect a significantly shorter decay time T_R for the sodium excitation than for the cesium excitation. In particular, an enhanced coupling due to decay channels at $k_{\parallel} \neq 0$ might again be crucial.⁴⁷ Our results for Na and Cs/Cu(100) support the conclusion that adsorbate-substrate separation has a considerable effect on the decay dynamics of adsorbate excitations. In addition, the missing difference between the autocorrelation trace of sodium and the clean Cu(100) surface suggests quite a strong coupling of the excited resonance state with the substrate as expected from the adsorption site of the sodium.

No clear conclusion is allowed about the lifetime results for Cs/Ag(111), as we only have proven knowledge about the lower limit of T_R . Considering the points mentioned in the discussion above, the detection of a lifetime comparable to that observed for Cs/Cu(111) would not be surprising. The properties assumed to be responsible for the coupling and decoupling of an adsorbate state are quite similar for both systems. For example, the sp band gap for Ag(111) extends from about 0.15 eV below E_F to about 3.9 eV above E_F at $k_{\parallel} = 0$,⁵⁴ quite close to the values for Cu(111). In addition, the closely packed surface structure suggests an identical adsorption geometry in comparison with Cs/Cu(111). More accurate results for Cs/Ag(111) would have given insight into the influence of the occupied d bands of the substrate. The energetical positions of these d bands differ by about 2 eV in both systems. Also, some dissimilarities due to the different radii of the substrate atoms might be expected. More extensive experiments would be desirable, e.g., by means of a two-color experiment.

The question arises of why no similar distinct lifetime effect could be detected for photoexcitation of CO (Refs. 13 and 16) absorbed on a Cu(111) and Cu(100) single-crystal surfaces. The conditions which probably give rise to a high resonance time also seem to be fulfilled for the CO adsorption system: The CO resonance—as investigated—is in any case located inside the band gap. Due to the low desorption temperature of CO of about 140 K the bonding between the substrate and CO is rather weak.

The key to an explanation for this might be the different symmetric character of the CO state compared to the alkali state. The dependence of the 2PPE intensity of this excitation on the laser polarization clearly indicates that for CO the orbital character is of π symmetry, as supposed to σ symmetry in the case of the alkalis.⁵⁵ As a consequence, it is likely that in addition to the decay channels almost perpendicular to the surface ($k_{\parallel}=0$), decay channels at $k_{\parallel}\neq 0$ outside the band gap become more important. This coupling to real states might significantly reduce the lifetime T_R of this excitation.

In summary, we have investigated the inelastic lifetime of a photoexcited electronic alkali state for cesium and sodium adsorbed on different noble-metal surfaces by means of a real-time experiment. The observed lifetime range from below our resolution of 4 fs for Na/Cu(100) up to 15 ± 6 fs for Cs/Cu(111). A hybrid character of the investigated state or/and the positioning of the excitation within a projected band gap might be possible explanations for the surprisingly high lifetimes. Both effects cause a strong decoupling from possible decay channels as offered by the bulk electronic structure of the substrate. In addition, our results clearly indicate that the adsorbate-substrate distance significantly affects the dynamical properties of the alkali excitation.

ACKNOWLEDGMENTS

We would like to thank M. Wolf, P. M. Echenique, and J. P. Gauyacq for helpful discussions. This work was supported by the Swiss National Science Foundation (Grant No. 21-39385.93).

*Present address: Center for Ultrafast Optical Science, University of Michigan, Ann Arbor, MI 48103.

[†]Present address: Institut für Laser- und Plasmaphysik, Universität Essen, D-45117 Essen, Germany.

¹J. W. Gadzuk, L. J. Richter, S. A. Buntin, and R. R. Cavanagh, *Surf. Sci.* **235**, 317 (1990); J. A. Misewich, T. F. Heinz, and D. M. Newns, *Phys. Rev. Lett.* **68**, 3737 (1992); S. M. Harris, S. Holloway, and G. R. Darling, *J. Chem. Phys.* **102**, 8235 (1995); J. W. Gadzuk, *Surf. Sci.* **342**, 345 (1995).

²W. Ho, *J. Phys. Chem.* **100**, 13 050 (1996).

³M. Asscher, F. M. Zimmermann, L. L. Springsteen, and P. L. Houston, *J. Chem. Phys.* **96**, 4808 (1992).

⁴F. J. Kao, D. G. Busch, D. Cohen, D. Comes da Costa, and W. Ho, *Phys. Rev. Lett.* **71**, 2094 (1993).

⁵J. A. Prybyla, H. W. K. Tom, and G. D. Aumiller, *Phys. Rev. Lett.* **68**, 503 (1992).

⁶R. Matzdorf, *Surf. Sci. Rep.* **30**, 153 (1998).

⁷Th. Fauster and W. Steinmann, in *Photonic Probes of Surfaces*, edited by P. Halevi, *Electromagnetic Waves: Recent Developments in Research Vol. 2* (North-Holland, Amsterdam, 1995), p. 347.

⁸H. Ueba, *Surf. Sci.* **334**, L719 (1995).

⁹R. W. Schoenlein, J. G. Fujimoto, G. L. Eesley, and T. W. Capehart, *Phys. Rev. Lett.* **22**, 2596 (1988).

¹⁰For an overview on the technique on TR-2PPE, see, e.g., H. Petek and S. Ogawa, *Prog. Surf. Sci.* **56**, 239 (1997).

¹¹M. Wolf, E. Knoesel, and T. Hertel, *Phys. Rev. B* **54**, R5295 (1996).

¹²R. W. Schoenlein, J. G. Fujimoto, G. L. Eesley, and T. W. Capehart, *Phys. Rev. Lett.* **22**, 2596 (1988).

¹³C. A. Schmittenmaer, M. Aeschlimann, J. W. Herman, R. J. D. Miller, D. A. Mantell, J. Cao, and Y. Gao, *Proc. SPIE* **2125**, 98 (1994).

¹⁴T. Hertel, E. Knoesel, M. Wolf, and G. Ertl, *Phys. Rev. Lett.* **76**, 535 (1996).

¹⁵U. Höfer, I. L. Shumay, Ch. Reuß, U. Thomann, W. Wallauer, and Th. Fauster, *Science* **277**, 1480 (1997).

¹⁶E. Knoesel, T. Hertel, M. Wolf, and G. Ertl, *Chem. Phys. Lett.* **240**, 409 (1995).

¹⁷M. Bauer, S. Pawlik, and M. Aeschlimann, *Surf. Sci.* **377–379**, 350 (1997).

¹⁸M. Bauer, S. Pawlik, and M. Aeschlimann, *Phys. Rev. B* **55**, 10 040 (1997).

¹⁹J. Bormet, J. Neugebauer, and M. Scheffler, *Phys. Rev. B* **49**, 17 242 (1994).

²⁰H. Ishida, *Phys. Rev. B* **39**, 5492 (1998).

²¹E. Knoesel, A. Hotzel, and M. Wolf, *J. Eng. Power* **88–91**, 577 (1998).

²²S. Ogawa, H. Nagano, H. Petek, and A. Heberle, *Phys. Rev. Lett.* **78**, 1339 (1997).

²³R. Loudon, *The Quantum Theory of Light* (Oxford University Press, Oxford, 1973).

²⁴A. Messiah, *Quantum Mechanics* (Wiley, New York, 1962), Vol. II.

²⁵M. Aeschlimann, M. Bauer, and S. Pawlik, *Chem. Phys.* **205**, 127 (1996).

²⁶D. Naumovic, P. Aebi, P. Stuck, P. Schwaller, J. Osterwalder, and L. Schlapbach, *Surf. Sci.* **307–309**, 483 (1994).

²⁷Q. B. Lu, D. J. O'Connor, B. V. King, and R. J. MacDonald, *Surf. Sci.* **347**, L61 (1996).

²⁸C. A. Papageorgopoulos, *Phys. Rev. B* **25**, 3740 (1982).

²⁹All coverage values are given with respect to a closely packed alkali layer at the substrate.

³⁰A. Kiejna and K. F. Wojciechowski, *Metal Surface Electron Physics* (Elsevier, Oxford, 1996).

³¹See, e.g., D. Heskett, K.-H. Frank, K. Horn, E. E. Koch, H.-J. Freund, V. Baddorf, K.-D. Tsuei, and E. W. Plummer, *Phys. Rev. B* **37**, 10 387 (1988); D. Tang and D. Heskett, *ibid.* **47**, 10 695 (1993); H. B. Nielsen and W. Thowladda, *Surf. Sci. Lett.* **284**, L426 (1993).

³²N. Fischer, S. Schuppler, Th. Fauster, and W. Steinmann, *Surf. Sci.* **314**, 89 (1994).

³³S. Reiff, W. Drachsel, and J. H. Block, *Surf. Sci. Lett.* **304**, L420 (1994).

³⁴D. A. Arena, F. G. Curti, and R. A. Bartynski, *Phys. Rev. B* **56**, 15 404 (1997); *Surf. Sci. Lett.* **369**, L117 (1996).

³⁵J. J. Quinn, *Phys. Rev.* **126**, 1453 (1962).

- ³⁶M. Aeschlimann, S. Pawlik, and M. Bauer, *Ber. Bunsenges. Phys. Chem.* **99**, 1504 (1995).
- ³⁷E. Knoesel, A. Hotzel, T. Hertel, M. Wolf, and G. Ertl, *Surf. Sci.* **368**, 76 (1996).
- ³⁸S. Ogawa, H. Nagano, and H. Petek, *Phys. Rev. B* **55**, 10 869 (1997).
- ³⁹M. Wolf, E. Knoesel, and T. Hertel, *Phys. Rev. B* **54**, R5295 (1996).
- ⁴⁰S. Pawlik, R. Burgermeister, M. Bauer, and M. Aeschlimann, *Surf. Sci.* **402–404**, 556 (1998).
- ⁴¹N. D. Lang and A. R. Williams, *Phys. Rev. B* **18**, 616 (1978).
- ⁴²P. Nordlander and J. C. Tully, *Phys. Rev. B* **42**, 5564 (1990).
- ⁴³A strong inhomogeneous (Gaussian) broadening of the alkali peak was reported before in Ref. 32, and is also observed in the present study.
- ⁴⁴L. Bartels, G. Meyer, K. H. Rieder, D. Velic, E. Knoesel, A. Hotzel, M. Wolf, and G. Ertl, *Phys. Rev. Lett.* **80**, 2004 (1998).
- ⁴⁵J. P. Muscat and D. M. Newns, *Surf. Sci.* **74**, 355 (1978).
- ⁴⁶V. Wertheim, D. M. Riffe, and P. H. Citrin, *Phys. Rev. B* **49**, 4834 (1994).
- ⁴⁷A. G. Borisov, A. K. Kazansky, and J. P. Gauyacq, *Surf. Sci.* **430**, 165 (1999).
- ⁴⁸M. Bauer, S. Pawlik, R. Burgermeister, and M. Aeschlimann, *Surf. Sci.* **404**, 62 (1998).
- ⁴⁹P. M. Echenique and J. B. Pendry, *Prog. Surf. Sci.* **32**, 111 (1990).
- ⁵⁰In detail, Fauster and Steinmann proposed multiplying this penetration factor by the lifetime of a bulk state at the same energy [see *Photonic Probes of Surfaces* (Ref. 7)].
- ⁵¹In theoretical calculations exactly this effect is supposed to be the reason for the observed difference in T_R between Cs and Li adsorbed on Cu(111) in the “zero”-coverage limit (Ref. 47). For the case of Li/Cu(111), these authors calculated that this effect could even overcompensate for an increase in the overall adsorbate substrate separation by a factor of 2.
- ⁵²At low coverages the alkali atom is supposed to be in a more or less positive ionic state [see *Metal Surface Electron Physics* (Ref. 30)].
- ⁵³J. Lehmann, P. Roos, and E. Bertel, *Phys. Rev. B* **54**, R2347 (1997).
- ⁵⁴K.-M. Ho, C.-L. Fu, S. H. Liu, D. M. Kolb, and G. Piazza, *J. Electroanal. Chem.* **150**, 235 (1983).
- ⁵⁵T. Hertel, E. Knoesel, E. Hasselbrink, M. Wolf, and G. Ertl, *Surf. Sci.* **317**, L1147 (1994).